Fusion Engineering and Design 146 (2019) 688–691

Contents lists available at ScienceDirect

Fusion Engineering and Design

journal homepage: www.elsevier.com/locate/fusengdes

Robust control of the current profile and plasma energy in EAST

Hexiang Wang*, Eugenio Schuster

Department of Mechanical Engineering and Mechanics, Lehigh University, Bethlehem, PA 18015, USA

ARTICLE INFO

Keywords:
Plasma control
Current profile control
Plasma stored energy control
Model-based control
Robust control
EAST

ABSTRACT

Integrated control of the toroidal current density profile, or alternatively the q-profile, and plasma stored energy is essential to achieve advanced plasma scenarios characterized by high plasma confinement, magnetohydrodynamics stability, and noninductively driven plasma current. The q-profile evolution is closely related to the evolution of the poloidal magnetic flux profile, whose dynamics is modeled by a nonlinear partial differential equation (PDE) referred to as the magnetic-flux diffusion equation (MDE). The MDE prediction depends heavily on the chosen models for the electron temperature, plasma resistivity, and non-inductive current drives. To aid control synthesis, control-oriented models for these plasma quantities are necessary to make the problem tractable. However, a relatively large deviation between the predictions by these control-oriented models and experimental data is not uncommon. For this reason, the electron temperature, plasma resistivity, and non-inductive current drives are modeled for control synthesis in this work as the product of an "uncertain" reference profile and a nonlinear function of the different auxiliary heating and current-drive (H&CD) source powers and the total plasma current. The uncertainties are quantified in such a way that the family of models arising from the modeling process is able to capture the q-profile and plasma stored energy dynamics from a typical EAST shot. A control-oriented nonlinear PDE model is developed by combining the MDE with the "uncertain" models for the electron temperature, plasma resistivity, and non-inductive current drives. This model is then rewritten into a control framework to design a controller that is robust against the modeled uncertainties. The resulting controller utilizes EAST's H&CD powers and total plasma current to regulate the q profile and plasma stored energy even when mismatches between modeled and actual dynamics are present. The effectiveness of the controller is demonstrated through nonlinear simulations.

1. Introduction

Ongoing work in the fusion community focuses on developing advanced plasma scenarios characterized by high plasma confinement, magnetohydrodynamic (MHD) stability, and noninductively driven plasma current. The toroidal current density profile, or alternatively the q-profile, together with the normalized beta (β_N) which is closely related to plasma energy, are often used to characterize these advanced scenarios. Having the capability of reproducing a particular combination of q-profile and β_N in spite of plasma and machine variability between discharges is thus critical to better study the associated plasma scenario. For this reason, different feedback control approaches such as [1–4] have been recently proposed to achieve this capability. All these control approaches are characterized by the use of a response model [5] due to the high dimensionality and nonlinearity of the to-be-controlled plasma dynamics.

In this work, an integrated controller for q-profile and plasma energy is designed for the EAST tokamak in P.R. China. The design is based on a first-principles-driven dynamic model of the poloidal magnetic profile evolution, which is governed by the magnetic-flux diffusion equation (MDE), and a power balance equation for plasma energy. Key components of the MDE such as electron temperature, plasma resistivity, and non-inductive current drives are modeled as the product of an "uncertain" reference profile and a nonlinear function of the different H&CD source powers and the total plasma current. These "uncertain" reference profile are modeled as the sum of a nominal profile and a bounded uncertainty. A response model suitable for the synthesis of a controller with tracking capabilities is obtained by reducing the dimensionality of the system via spatial discretization and by linearizing the dynamics around the to-be-tracked trajectory. A singular value decomposition [6] is applied to the linearized model to identify the most effective control channels and to decouple the model at steady state. A mixed sensitivity $\mathcal{H}_\infty$ control problem is then defined to synthesize a controller with the capability of tracking the desired trajectory with minimum control energy in presence of arbitrary initial conditions and disturbances. The robust stability of the closed-loop

* Corresponding author.
E-mail address: hexiang.wang@lehigh.edu (H. Wang).

https://doi.org/10.1016/j.fusengdes.2019.01.056
Received 5 October 2018; Received in revised form 21 December 2018; Accepted 10 January 2019
Available online 23 January 2019

system is verified through the computation of the structured singular values based on the modeled uncertainty.

This paper is organized as follows. In Section 2, the MDE and the power balance equation are given. Uncertainty-based models together with a model reduction strategy are provided in Section 3. Formulation of the mixed sensitivity $\mathcal{H}_\infty$ control problem is given in Section 4. The result of a simulation case showing the effectiveness of the robust controller is presented in Section 5. In Section 6, conclusions and future work are stated.

2. Poloidal magnetic flux and energy evolution models

Any quantity constant on each magnetic surface could be chosen as an indexing coordinate ρ. We choose the mean effective minor radius of the magnetic surface as the variable ρ, i.e., $\pi B_{\phi,0}\rho^2 = \Phi$, where Φ is the toroidal magnetic flux and $B_{\phi,0}$ is the toroidal magnetic field at the major radius of the device, R_0. The normalized effective minor radius $\hat{\rho}$ is defined as $\hat{\rho} = \rho/\rho_b$, where ρ_b is the mean effective minor radius of the uttermost closed magnetic flux surface. The evolution of the poloidal magnetic flux is given by the MDE,

$$\frac{\partial \psi}{\partial t} = \frac{\eta(T_e)}{\mu_0 \rho_b^2 \hat{F}^2}\frac{1}{\hat{\rho}}\frac{\partial}{\partial \hat{\rho}}\left(\hat{\rho} D_\psi \frac{\partial \psi}{\partial \hat{\rho}}\right) + R_0 \hat{H}\eta(T_e)\frac{\langle \bar{j}_{\mathrm{NI}}\cdot\bar{B}\rangle}{B_{\phi,0}}, \tag{1}$$

where ψ is the poloidal flux per radian, which is closely related to the poloidal flux Ψ, i.e. $\Psi = 2\pi\psi$, t is the time, η is the plasma resistivity, T_e is the electron temperature, μ_0 is the vacuum permeability, $\langle \bar{j}_{\mathrm{NI}}\cdot\bar{B}\rangle/B_{\phi,0}$ is the non-inductive current drive and $D_\psi(\hat{\rho}) = \hat{F}(\hat{\rho})\hat{G}(\hat{\rho})\hat{H}(\hat{\rho})$. $\hat{F}(\hat{\rho})$, $\hat{G}(\hat{\rho})$, $\hat{H}(\hat{\rho})$ are geometric factors pertaining to the magnetic configuration of a particular plasma equilibrium. The boundary conditions are given by $\partial\psi/\partial\hat{\rho}|_{\hat{\rho}=0} = 0$, $\partial\psi/\partial\hat{\rho}|_{\hat{\rho}=1} = -\mu_0 R_0 I_p/(2\pi\hat{G}(1)\hat{H}(1))$, where I_p is the total plasma current. The evolution of the volume-averaged energy is modeled as,

$$\frac{\mathrm{dW}}{\mathrm{dt}} = -\frac{W}{\tau_E(t)} + P_{\mathrm{tot}}(t), \tag{2}$$

where τ_E is the global energy confinement time, which is modeled based on the scaling law $IPB98(y, 2)$ [7], and $P_{tot}(t) = P_{ohm}(t) + P_{aux}(t) - P_{rad}(t)$ is the total power injected into the plasma. $P_{ohm}(t)$ is the ohmic power, $P_{aux}(t)$ is the heating and current-drive (H&CD) power, and $P_{rad}(t)$ is the radiated power. On EAST, we have $P_{\mathrm{aux}}(t) = P_{\mathrm{nbi}_1}(t) + P_{\mathrm{nbi}_2}(t) + P_{\mathrm{nbi}_3}(t) + P_{\mathrm{nbi}_4}(t) + P_{\mathrm{lh}}(t) + P_{\mathrm{ich}}(t)$. $P_{\mathrm{nbi}_1}(t)$ and $P_{\mathrm{nbi}_2}(t)$ are the powers of the two co-current neutral beam injection (NBI) sources, $P_{\mathrm{nbi}_3}(t)$ and $P_{\mathrm{nbi}_4}(t)$ are the powers of the two counter-current NBIs. While there are two lower-hybrid (LH) sources in EAST (2.45 GHz and 4.6 GHz), only the 4.6 GHz launcher is considered in this work and its associated power is denoted by $P_{lh}(t)$. Finally, $P_{ich}(t)$ is the power of the ion cyclotron (IC) source. The non-inductive current drive can be modeled as

$$\frac{\langle \bar{j}_{\mathrm{NI}}\cdot\bar{B}\rangle}{B_{\phi,0}} = \sum_{j=1}^{4} j_{\mathrm{nbi}_j}(\hat{\rho}, t) + j_{\mathrm{lh}}(\hat{\rho}, t) + j_{\mathrm{bs}}(\hat{\rho}, t). \tag{3}$$

where $j_{\mathrm{nbi}_j}(\hat{\rho}, t)$, for $j = 1, \ldots 4$, and $j_{\mathrm{lh}}(\hat{\rho}, t)$ represent the non-inductive current driven by the NBI and LH sources, which are modeled following [5]. The bootstrap current j_{bs} is modeled as

$$j_{\mathrm{bs}}(\hat{\rho}, t) = \frac{R_0}{\hat{F}(\hat{\rho})}\left(\frac{\partial\psi}{\partial\hat{\rho}}\right)^{-1}\left[\mathcal{L}_1(\hat{\rho})T_e\frac{\partial n_e}{\partial\hat{\rho}} + \mathcal{L}_2(\hat{\rho})n_e\frac{\partial T_e}{\partial\hat{\rho}}\right], \tag{4}$$

where electron and ion densities and temperatures are assumed identical (i.e., $T_e = T_i$ and $n_e = n_i$) and are modeled following [5]. The coefficients $\mathcal{L}_1(\hat{\rho})$ and $\mathcal{L}_2(\hat{\rho})$ depend on the magnetic configuration of a particular plasma equilibrium [8]. The current driven by the IC source is considered negligible.

3. Uncertainty-based model for robust control synthesis

The electron temperature, plasma resistivity, and non-inductive current drives are re-modeled for control synthesis purposes. Defining $f(\hat{\rho}, t) \in \{T_e, \eta, j_{\mathrm{lh}}, j_{\mathrm{nbi}_j}\}$, f is modeled as

$$f(\hat{\rho}, t) = f_s(\hat{\rho})f_t(t), \tag{5}$$

$$f_s(\hat{\rho}) = f^{\mathrm{nom}}(\hat{\rho}) + f^{\mathrm{unc}}(\hat{\rho})\delta_f, \quad |\delta_f| \le 1, \tag{6}$$

$$f^{\mathrm{nom}}(\hat{\rho}) = \frac{f^{\max} + f^{\min}}{2}, \quad f^{\mathrm{unc}}(\hat{\rho}) = \frac{f^{\max} - f^{\min}}{2}, \tag{7}$$

$$f^{\max} = \max_t \frac{f(\hat{\rho}, t)}{f_t(t)}, \quad f^{\min} = \min_t \frac{f(\hat{\rho}, t)}{f_t(t)}. \tag{8}$$

The plasma resistivity is a monotonically decreasing function of the electron temperature. In this work, $\delta_\eta = \delta_{T_e}$ is adopted and the definition of f^{unc} is pre-multiplied by a negative sign when computing η^{unc}. By defining $u_{T_e} \triangleq I_p^\alpha P_{\mathrm{tot}}^\gamma \bar{n}_e^\zeta$, where $\bar{n}_e$ is the line-average density and the parameters α, γ, ζ can be deduced from the scaling law for τ_E, it is possible to write

$$\begin{aligned}
&f_t(t) = u_{T_e}(t), f \in \{T_e\}, f_t(t) = u_{T_e}(t)^{-1.5}, f \in \{\eta\},\\
&f_t(t) = u_{T_e}(t)P_{\mathrm{lh}}(t)\bar{n}_e(t)^{-1}, f \in \{j_{\mathrm{lh}}\},\\
&f_t(t) = \sqrt{u_{T_e}(t)}P_{\mathrm{nbi}_j}(t)\bar{n}_e(t)^{-1}, f \in \{j_{\mathrm{nbi}_j}\}, j \in [1, 2, 3, 4].
\end{aligned}$$

The ranges of uncertainty for the electron temperature, plasma resistivity, and lower hybrid current drive are shown in Fig. 1. No uncertainty is finally considered in this work for the NBI current drives, i.e. $\delta_{\mathrm{nbi}_j} \equiv 0, j \in [1, 2, 3, 4]$.

Since the q-profile is inversely proportional to the gradient of the poloidal magnetic flux θ, where $\theta \triangleq \partial\psi/\partial\hat{\rho}$, (1) is differentiated with respect to $\hat{\rho}$ to obtain a PDE in θ. By defining the control input as $u = [I_p, P_{\mathrm{nbi}_1}, P_{\mathrm{nbi}_2}, P_{\mathrm{nbi}_3}, P_{\mathrm{nbi}_4}, P_{\mathrm{lh}}, P_{\mathrm{ich}}]$, and the uncertainty vector as $\delta = [\delta_{T_e}, \delta_{j_{\mathrm{lh}}}]$, this PDE is written as

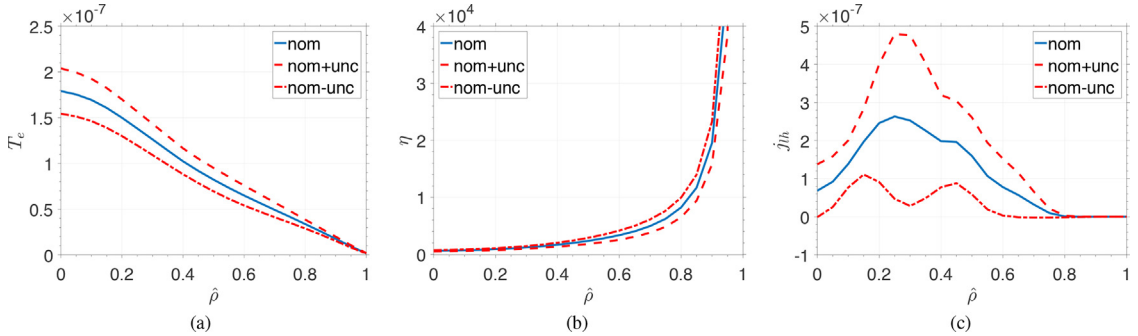

Fig. 1. Model uncertainty ranges: (a) electron temperature $(\mathrm{keV/A^{0.93}/W^{0.31}/(10^{19}/m^3)^{-0.59}})$, (b) plasma resistivity $(\Omega\,\mathrm{m\,A^{1.395}\,W^{0.465}(10^{19}/m^3)^{-0.885}})$, (c) non-inductive current driven by 4.6 GHz LH source $(\mathrm{A^{0.07}/m^2/W^{1.31}/(10^{19}/m^3)^{-1.59}})$. The nominal profiles are representative EAST profiles (shot #73690).

$$\dot{\theta} = g\left(\theta, \frac{\partial\theta}{\partial\hat{\rho}}, \frac{\partial^2\theta}{\partial\hat{\rho}^2}, u, \delta\right) \tag{9}$$

To reduce the infinite dimensionality of (9) both for control synthesis and simulation, the spatial domain is discretized via a finite difference method. Furthermore, by choosing the state $Z = [\theta(\hat{\rho}_i, t), W]$, $i = [2, \cdots, n-1]$, where n is the number of points in the spatial grid, an augmented model that combines (2) and (9) is written as $\dot{Z} = F(Z, u, \delta)$. To facilitate the synthesis of a tracking-capable controller, the model is further reduced by linearization around a given trajectory (Z_{ff}, u_{ff}) satisfying $\dot{Z}_{\mathrm{ff}} = F(Z_{\mathrm{ff}}, u_{\mathrm{ff}}, \mathbf{0})$. By defining $\tilde{Z} = Z - Z_{\mathrm{ff}}$, $u_{\mathrm{fb}} = u - u_{\mathrm{ff}}$ and neglecting higher-order terms, the model is written as

$$\dot{\tilde{Z}} = A\tilde{Z} + \mathrm{B}u_{\mathrm{fb}} + d,\ y = C\tilde{Z} + D, \tag{10}$$

where $A = \partial F/\partial Z|_{(Z_{\mathrm{ff}}, u_{\mathrm{ff}}, \mathbf{0})}$, $B = \partial F/\partial u|_{(Z_{\mathrm{ff}}, u_{\mathrm{ff}}, \mathbf{0})}$, $d = F(Z_{ff}, u_{ff}, \delta) - F(Z_{ff}, u_{ff}, \mathbf{0})$, $A = A_0 + A_1\delta_{T_e} + A_2\delta_{j_{\mathrm{lh}}}$, $B = B_0 + B_1\delta_{T_e} + B_2\delta_{j_{\mathrm{lh}}}$, $C = I_{n-1}$, and $D = \mathbf{0}$.

4. Formulation of mixed sensitivity $\mathcal{H}_\infty$ control problem

Since (10) represents an underactuated system, a singular value decomposition of a weighted transfer function G_{ss} for the nominal system A_0, B_0, C, D at steady state is employed, i.e.

$$\bar{y} = G_{\mathrm{ss}}\bar{u}_{\mathrm{fb}},\ G_{\mathrm{ss}} = -\mathrm{C}A_0^{-1}B_0,\ \mathrm{USV}^T = Q^{1/2}G_{\mathrm{ss}}R^{-1/2}, \tag{11}$$

where $\bar{y}$ and $\bar{u}_{\mathrm{fb}}$ are the system output and input at steady state, and $Q \in \mathbb{R}^{(n-1)\times(n-1)}$ and $R \in \mathbb{R}^{7\times7}$ are two positive definite weighting matrices. $S = diag(\sigma_1, \sigma_2, \cdots, \sigma_6, \sigma_7)$, where σ_i, for $i = 1, \ldots, 7$, are the singular values of G_{ss}. The columns of $U \in \mathbb{R}^{(n-1)\times7}$ and $V \in \mathbb{R}^{7\times7}$ are left and right singular vectors respectively. By partitioning U, S, V into $[U_p, U_n]$, $diag(S_p, S_n)$, and $[V_p, V_n]$ respectively, where $S_p \in \mathbb{R}^{l\times l}$ and $S_n \in \mathbb{R}^{(7-l)\times(7-l)}$, (11) can be rewritten as

$$\bar{y} = Q^{-1/2}\mathrm{USV}^TR^{1/2}\bar{u}_{\mathrm{fb}} \approx Q^{-1/2}U_pS_pV_p^TR^{1/2}\bar{u}_{\mathrm{fb}}. \tag{12}$$

The notation $(\cdot)_p$ and $(\cdot)_n$ has been used to represent the most effective (primary) and less effective (negligible) control directions. By defining $\hat{y} = S_p^{-1}U_p^TQ^{1/2}\bar{y}$ and $\hat{u}_{\mathrm{fb}} = V_p^TR^{1/2}\bar{u}_{\mathrm{fb}}$, a decoupled system at steady state is obtained, i.e.

$$\hat{y} = \hat{u}_{\mathrm{fb}}. \tag{13}$$

In this work, $l = 3$ is chosen. More details regarding this technique can be found in [9].

4.1. Mixed sensitivity $\mathcal{H}_\infty$ control problem formulation

The basic idea of the mixed-sensitivity $\mathcal{H}_\infty$ control synthesis procedure is to find a controller K such that the $\mathcal{H}_\infty$ norm of a chosen closed-loop transfer function is minimized. By using the singular value decomposition introduced in (12), it is possible to define $\hat{e} = \hat{r} - \hat{y} = S_p^{-1}U_p^TQ^{1/2}(r - y)$ and $\hat{u}_{\mathrm{fb}} = V_p^TR^{1/2}u_{\mathrm{fb}}$ as shown in Fig. 3, where u_d represents the input disturbance, r is the to-be-tracked reference, ω_P and ω_u are weight transfer functions, and $\Delta = \mathrm{diag}(\delta_{T_e}, \delta_{j_{\mathrm{lh}}})$ is the structured uncertainty. Note that the model is rewritten into a general $P - \Delta$ control configuration including model uncertainty. Details on how to rewrite the model into this configuration can be found in [6]. In this work, the objective is to minimize a weighted version of the tracking error $\hat{e}$ (i.e., $z_1 = \omega_p\hat{e}$) and a weighted version of the control effort $\hat{u}_{\mathrm{fb}}$ (i.e., $z_2 = \omega_u\hat{u}_{\mathrm{fb}}$). The problem can then be formulated as

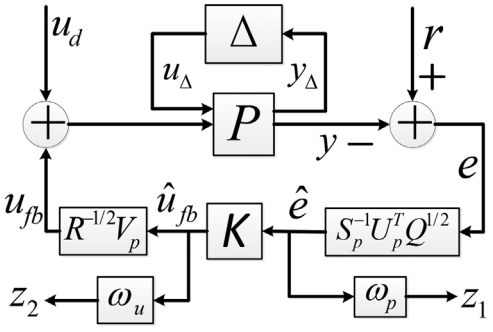

Fig. 3. $\mathcal{H}_\infty$ control scheme.

$$\min_K \|N(K)\|_\infty,\ \text{where}\ N = \begin{bmatrix} \omega_P S \\ \omega_u \mathrm{KS} \end{bmatrix}, \tag{14}$$

and the $\mathcal{H}_\infty$ of N is computed as $\|N\|_\infty = \max_\omega \bar{\sigma}(N(j\omega))$, where $\bar{\sigma}(N(j\omega))$ represents the maximum singular value of the matrix $N(j\omega)$. The closed-loop transfer function from r to Z_1 is given by ω_pS while the closed-loop transfer function from r to Z_2 is given by ω_uKS, where $S = [I_3 + S_p^{-1}U_p^TQ^{1/2}C(\mathrm{s}I_{n-1} - A_0)^{-1}B_0R^{-1/2}V_pK]^{-1}$ is the closed-loop sensitivity function. Therefore, by minimizing the maximum gain over frequency of the transfer function N, both the weighted tracking error Z_1 and the weighted control effort Z_2 are minimized for any arbitrary reference r. In this work, ω_p and ω_u are defined as

$$\omega_P = \mathrm{diag}(\omega_{P_1}, \omega_{P_2}, \omega_{P_3}), \quad \omega_u = \mathrm{k}I_3, \tag{15}$$

$$\omega_{P_i} = \frac{s/M_i + \omega_{c_i}}{s + \omega_{c_i}N_i}, \quad i = 1, \ldots, 3. \tag{16}$$

where k, M_i, ω_{c_i}, N_i are design parameters. The controller for the original system ($u_{fb} = K_re$) can be finally written as

$$K_r = R^{-1/2}V_p\mathrm{K}S_p^{-1}U_p^TQ^{1/2}. \tag{17}$$

Once the controller is designed, the closed-loop model can be rewritten into a $M\Delta$-structure for robust stability analysis [6]. In this case, the structured singular value is confirmed to be less than 1, which guarantee robust stability (i.e., closed-loop stability for all the family of "uncertain" models).

5. Nonlinear closed-loop simulation study

The proposed controller (17) has been tested through simulations based on the nonlinear model (1)–(2). The models used in the simulation study for the electron temperature, the plasma resistivity, and the non-inductive current driven by the 4.6GHz LH source follow [5], and not the uncertain model (5)–(8), which has only been used to design the controller. Additionally, perturbed initial conditions in θ and input disturbances are introduced in the simulations. The disturbances are defined as $u_{d,I_p} = 0.04$ MA, $u_{d,P_{\mathrm{nbi}_1}} = 0.5$ MW, $u_{d,P_{\mathrm{nbi}_3}} = 0.5$ MW, $u_{d,P_{\mathrm{nbi}_4}} = 0.8$ MW, $u_{d,P_{\mathrm{lh}}} = -0.5$ MW, $u_{d,P_{\mathrm{ich}}} = 0.5$ MW. Fig. 2 compares the q profile and W obtained in feedforward-only and feedforward + feedback simulations. The corresponding control inputs are also shown in the figure. For $t < 2s$, the feedback controller is off and both q and W evolve from the perturbed initial conditions driven by the feedforward control inputs. At $t = 2$ s, the feedback controller is turned on and both q and W immediately start tracking their respective targets in the feedforward + feedback simulation case. At $t = 2.5s$, the input disturbances are injected. While q and W diverge even further from the targets in the feedforward-only simulation case, tracking of the targets is recovered shortly after the transient introduced by the perturbations in the feedforward + feedback case.

6. Conclusions and future work

A model-based controller for the gradient of the poloidal magnetic flux profile and the plasma stored energy has been proposed for EAST by employing a mixed sensitivity $\mathcal{H}_\infty$ control design approach. The controller is designed to track any set of achievable target trajectories in presence of model uncertainties, initial state perturbations, and input disturbances. A novel way of modeling the electron temperature,

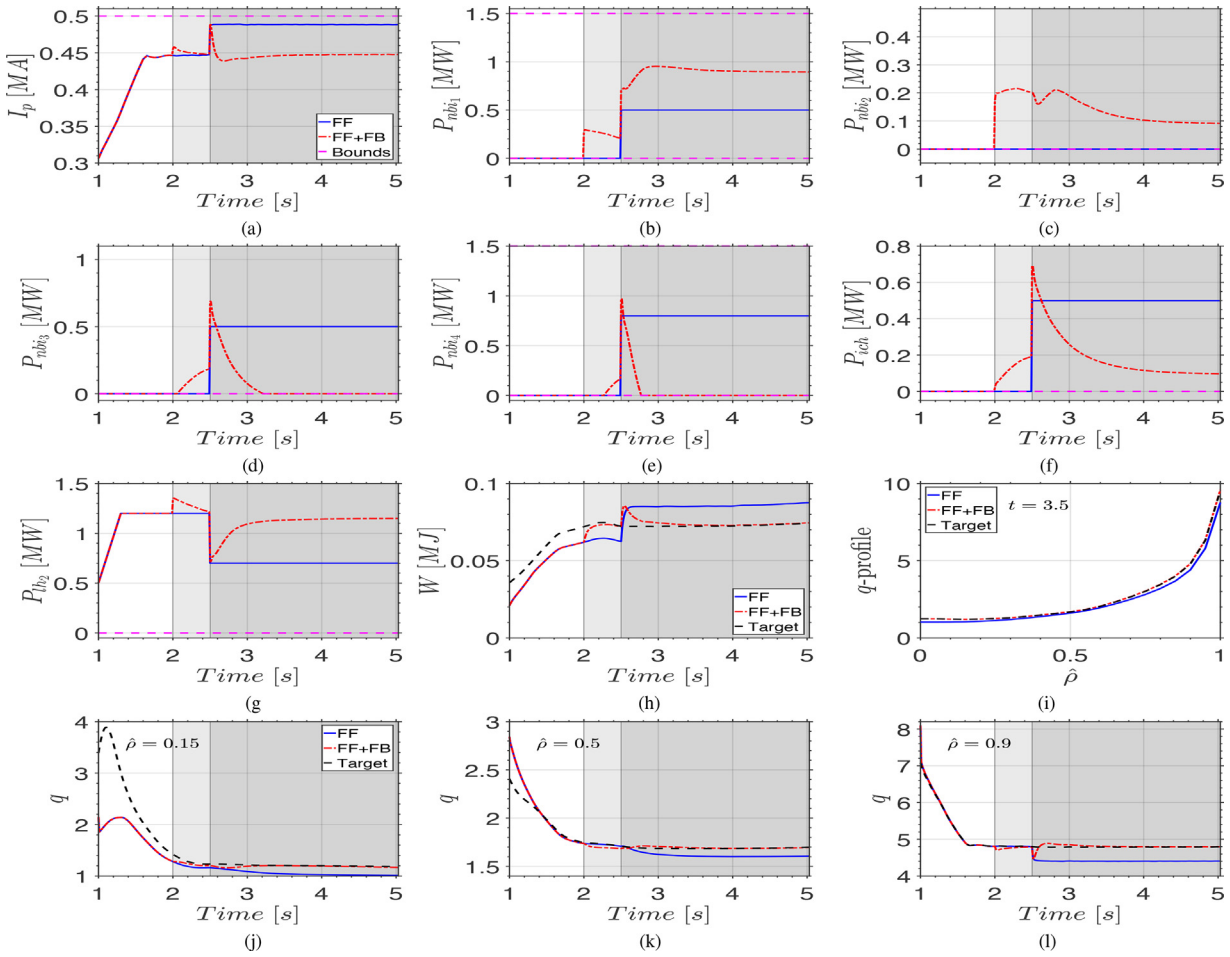

Fig. 2. Closed-loop simulation results for robust controller: (a)–(g) actuator trajectories, (h) W time evolution, (i) q profile at $t = 3.5$ s, (j)–(l) q time evolution at different $\hat{\rho}$ values. White region: feedback off, disturbances off; light-gray region: feedback on, disturbances off; dark-gray region: feedback on, disturbances on.

plasma resistivity, and non-inductive current drives has been introduced for the purpose of robust control synthesis. The approach explicitly takes into account uncertainties in the profiles while respecting widely accepted physics-based correlations for these models. Nonlinear simulation results illustrate the effectiveness of the controller and its readiness for experimental testing on EAST.

Acknowledgement

Work supported by the US DoE (DE-SC0010537).

References

[1] Y. Ou, C. Xu, E. Schuster, T.C. Luce, J.R. Ferron, M.L. Walker, D.A. Humphreys, Receding-horizon optimal control of the current profile evolution during the ramp-up phase of a tokamak discharge, Control Eng. Pract. 19 (1) (2011) 22–31.

[2] J. Barton, M. Boyer, W. Shi, E. Schuster, others, Toroidal current profile control during low confinement mode plasma discharges in DIII-D via first-principles-driven model-based robust control synthesis, Nucl. Fusion 52 (2012) 123018 (24pp).

[3] E. Maljaars, et al., Control of the tokamak safety factor profile with time-varying constraints using MPC, Nucl. Fusion 55 (2015) 023001 (18pp).

[4] M.D. Boyer, J.E. Barton, E. Schuster, et al., Backstepping control of the toroidal plasma current profile in the DIII-D tokamak, IEEE Trans. Control Syst. Technol. 22 (5) (2014) 1725–1739.

[5] Y. Ou, et al., Towards model-based current profile control at DIII-D, Fusion Eng. Des. 82 (5-14) (2007) 1153–1160.

[6] S. Skogestad, I. Postlethwaite, Multivariable Feedback Control Analysis and Design, Wiley, 2005.

[7] ITER EDA, et al., ITER Physics Basis Editors, Nucl. Fusion 39 (12) (1999) 2201–2215.

[8] O. Sauter, et al., Neoclassical conductivity and bootstrap current formulas for general axisymmetric equilibria and arbitrary collisionality regime, Phys. Plasmas 6 (7) (1999) 2834.

[9] J.E. Barton, K. Besseghir, J. Lister, E. Schuster, Physics-based control-oriented modeling and robust feedback control of the plasma safety factor profile and stored energy dynamics in ITER, Plasma Phys. Controll. Fusion 57 (2015) 115003 29pp..